Analytical solutions for the electromagnetic fields of flattened and annular Gaussian laser modes. I. Small *F*-number laser focusing

Scott M. Sepke and Donald P. Umstadter

Department of Physics and Astronomy, University of Nebraska, Lincoln, Nebraska 68588-0111

Received March 14, 2006; accepted June 2, 2006; posted June 22, 2006 (Doc. ID 68842)

Many laser interaction models assume that incident focused laser fields are Gaussian and use either the approximate TEM_{00} series model or the exact integral Gaussian angular-spectrum solution. Many practical laser systems, however, produce flat-top transverse intensity profiles, and indeed, such profiles are often desired. Here, an exact, integral solution is derived for all of the vector components having a general flattened Gaussian profile using the angular-spectrum method. This solution includes the pure and annular Gaussian modes as special cases. The resulting integrals are solved for tight focusing conditions exactly by making use of a Fourier–Gegenbauer expansion. This technique follows closely that of Sepke and Umstadter [Opt. Lett. **31**, 1447 (2006)] but, by redefining the expansion coefficients, the simplicity of the model is greatly enhanced and the computation time reduced by roughly a factor of 2 beyond the 2 orders of magnitude improvement obtained previously. This series solution is stable at all points and converges after $S \sim 20w_0$ terms, where w_0 is the $1/e$ waist normalized to the laser wavelength. © 2006 Optical Society of America

OCIS codes: 140.3300, 260.2110, 350.5500.

1. INTRODUCTION

When investigating any laser interaction, an accurate description of the electromagnetic fields is essential. As field intensities rise and focusing approaches the laser wavelength, plane wave and even paraxial formulations fail to capture all of the relevant physics. This has been analyzed in great detail by Hora and colleagues for many years: the so-called nonlinearity principle.[1–4] The importance of the physical model of focused laser fields has been extensively illustrated in direct laser–electron scattering, for example, by Cicchitelli *et al.*[1] in analyzing the ionization experiments of Boreham and Luther-Davíes[5] and Boreham and Hora,[6] and also more recently, both experimentally and theoretically in Refs. 6–11. As even small field corrections significantly affect the ponderomotive deflection, accurate field models that capture all of the detail within each component are required.

Often, laser fields are assumed to be nominally Gaussian. Paraxial Gaussian fields are well established, and their derivation and character have been described in great detail, for example, by Siegman.[12] Longitudinal corrections to this solution were first described by Lax, *et al.*,[13] and this work was quickly followed by that of Davis[14] and Hora,[2] who extended the formalism and solidified the relation to laser fields. These nonparaxial solutions have since been extended by Barton and Alexander,[15] Wang *et al.*,[16] and many others. The Maxwell wave equation has also been solved using Fourier transforms, yielding a formally exact solution for a Gaussian laser by Cicchitelli *et al.*[1] and later by Quesnel and Mora[8] and Varga and Török.[17] Although this has led to a detailed knowledge of focused Gaussian laser fields, vector field models for flat-top laser beams have received much less attention.

Although approximating a laser field as Gaussian is often a reasonable and accurate assertion, such a Gaussian model is in fact an idealization. Focusing optics or amplification of the laser pulse in practical situations often lead to a flat-top laser profile. Indeed, in many instances, a flattened profile is desired, as many applications require such a profile, including laser-induced plasma shocks,[18] electron acceleration,[19] photolithography,[20] laser chemical-vapor deposition,[20] and coherent data processing.[21] A large body of work exists in the optics literature on both paraxial and nonparaxial approximate solutions[22–25] for these fields, as well as methods of generating them.[26–29] A niche has also been found for annular laser modes,[16,30–33] having applications in such areas as laser machining and atom trapping,[34] as well as the stimulation of pain in neurological research.[35]

Heretofore, flat-top laser models have concentrated on scalar models used to describe their paraxial propagation, and several different formalisms have been used: super-Gaussians,[36] weighted sums of Gaussians having different focusing parameters,[24,25,37,38] the forms $(1-r^2)^{1/\gamma}\,\mathrm{rect}(r-1/2)$ and $\{1+\exp[\gamma(r-1)]\}^{-1}$ $\{\gamma \in \mathbb{Z}\}$ described by Gori,[39] a super-Lorentzian,[24] wavelets,[40] and the flattened Gaussian introduced by Gori[39] and utilized by Santarsiero and Borghi[41] and Bagin *et al.*[42] All of these have been used to describe the scalar/paraxial properties of flat-top fields and are suitable, in principle, to generate a full vector theory for a flattened/annular focused laser beam. In fact, an exact analytical vector solution has been recently derived for a flattened Gaussian[43] using the angular spectrum of the plane-wave technique.[44,45] This solution, however, is complicated and cumbersome to implement.

In this paper, following the model of Ref. 43, an *exact* vector integral solution to the full Maxwell wave equation is derived for a laser having a flattened Gaussian transverse profile in the focal plane using Fourier transforms by the angular spectrum of the plane-wave method.[44,45] The general nature of the formal prototype boundary condition used allows for a great amount of flexibility and even control of the size and complexity of the computations in modeling realistic field distributions. This technique has also been employed in the optics literature, for example, by Agrawal and Pattanayak[46] to model unpolarized light and by Cicchitelli *et al.*[1] and later by Quesnel and Mora[8] and Varga and Török[17] to compute the field components of a purely Gaussian beam. Borghi *et al.* also calculated the asymmetric electric field along the laser axis in this way for both Gaussian and flattened Gaussian distributions assuming loose focusing.[22]

The integrals resulting from this derivation are in the form of Gegenbauer's finite integral and under tight focusing conditions—that is, when the laser spot size w_0 is less than ~20 wavelengths—can be evaluated exactly following the model of Watson[47] or Kant.[48] This has, in fact, been done recently by beginning with the asymmetric field integrals.[43] Here, the symmetric field integrals are solved analytically, taking full advantage of the formal symmetry of the integrands, thereby greatly simplifying the final expressions for the field components and decreasing the computational effort required. Once the model is complete, the application to large scale calculations is described. The form of this solution lends itself well to the application of solving boundary value problems such as in particle-in-cell codes. The range of applicability and stability are also discussed, and some important limits are considered. In fact, the Gegenbauer polynomial series used in this solution converges faster as the laser spot size approaches the wavelength, in direct contrast to the standard perturbative Gaussian solutions described above, making this an attractive alternative when tightly focused fields are required.

2. EXACT INTEGRAL FLAT-TOP SOLUTION

A powerful technique for solving the Maxwell wave equation is the angular-spectrum method. In this technique, propagating electromagnetic fields are decomposed into a continuous sum of plane waves traveling at angles ranging from 0 to $\pi/2$ relative to the propagation axis. By evaluating the Fourier and subsequent inverse Fourier transform of a specified boundary condition, all six of the field components are calculated in all space.[44,45] This is an attractive method, as the result is an exact solution to Maxwell's equations that captures nonconstant transverse field distributions. Plane waves are, of course, also exact but are infinite in extent and, hence, physically unrealistic. Conversely, the Hermite–Gaussian modes and their lowest-order paraxial terms are solutions that capture realistic focusing but are only approximations.

To derive the asymmetric laser field solution, the transverse field distribution in the focal plane $z=0$ is formally specified: $E_x(x,y,z=0)$. This is then Fourier transformed in both transverse dimensions,

$$A_x(p,q) = \frac{1}{\lambda_0^2}\int\int_{\mathbb{R}^2} E_x(x,y,z=0)e^{-ik_0(px+qy)}\mathrm{d}x\mathrm{d}y,$$

and this transform is then inverted,

$$E_x^a(x,y,z) = \int\int_{\mathbb{R}^2} A_x(p,q)e^{ik_0(px+qy+mz)}\mathrm{d}p\mathrm{d}q,$$

where $m=(1-p^2-q^2)^{1/2}$ is the longitudinal direction cosine of the outgoing plane waves, $k_0=2\pi/\lambda_0$ is the wavenumber, and the $\exp[-i(\omega_0 t+\phi_0)]$ time dependence has been suppressed. As the field is plane polarized, the electric field component $E_y\equiv 0$, and the remaining field components are

$$E_z^a = i\partial_{\bar{x}}\int\int_{\mathbb{R}^2} A_x(p,q)\frac{e^{ik_0(px+qy+mz)}}{m}\mathrm{d}p\mathrm{d}q, \tag{1}$$

$$B_x^a = i\partial_{\bar{x}\bar{y}}^2\int\int_{\mathbb{R}^2} A_x(p,q)\frac{e^{ik_0(px+qy+mz)}}{m}\mathrm{d}p\mathrm{d}q, \tag{2}$$

$$B_y^a = \int\int_{\mathbb{R}^2} A_x(p,q)me^{ik_0(px+qy+mz)}\mathrm{d}p\mathrm{d}q - \partial_{\bar{x}}^2\int\int_{\mathbb{R}^2} A_x(p,q)\frac{e^{ik_0(px+qy+mz)}}{m}\mathrm{d}p\mathrm{d}q, \tag{3}$$

$$B_z^a = i\partial_{\bar{y}}\int\int_{\mathbb{R}^2} A_x(p,q)e^{ik_0(px+qy+mz)}\mathrm{d}p\mathrm{d}q, \tag{4}$$

where $\partial_{\bar{a}}=k_0^{-1}\partial_a$. The fully symmetric solution is then found by repeating this calculation with $B_y(z=0)$ and $B_x\equiv 0$ specified and averaging the two results.

Cicchitelli *et al.*,[1] Quesnel and Mora,[8] and Varga and Török[17] have derived an exact laser field model in this way by imposing a Gaussian field boundary condition in the focal plane; that is, $E_x(z=0)=E_0\exp(-r^2/w_0^2)$, where $r^2=x^2+y^2$ and w_0 is the waist. Here, consider the more-general flattened Gaussian distribution,

$$E_x(x,y,z=0) = E_0\sum_{N=0}^{\infty} A_N\left(\frac{r^2}{w_0^2}\right)^N e^{-(r^2/w_0^2)}, \tag{5}$$

where the parameters A_N are a set of arbitrary constants describing the detailed structure of the laser profile. Note that this reduces to the Gaussian case for $A_0=1$ and $A_{N>0}=0$. The Fourier transform follows as

$$A_x(p,q) = \left(\frac{E_0}{\pi\epsilon^2}\right)e^{-(b^2/\epsilon^2)}\sum_{N=0}^{\infty} A_N N! L_N\left(\frac{b^2}{\epsilon^2}\right),$$

where $b^2=p^2+q^2$, $\epsilon=2/k_0w_0$, and $L_N(x)$ is the Nth-order unassociated Laguerre polynomial. Converting to polar coordinates such that $p=b\cos\theta$ and $q=b\sin\theta$ and carrying out the azimuthal integration,

$$E_x^a = \sum \int_0^1 e^{-(b^2/\epsilon^2)} e^{imk_0 z} J_0(k_0 r b) L_N\left(\frac{b^2}{\epsilon^2}\right) b\,\mathrm{d}b,$$

where $J_n(x)$ is the nth order Bessel function of the first kind, and Σ denotes $2\epsilon^{-2}E_0\Sigma_{N=0}^{\infty}A_N N!$ throughout. The upper bound of integration has been restricted by the radiation condition, meaning that only forward-propagating plane waves contribute to the final beam; evanescent waves do not.[45] From Eqs. (1)–(4), then, the remaining asymmetric field components follow as

$$E_z^a = i \sum \partial_{\bar{x}} \int_0^1 e^{-(b^2/\epsilon^2)} \frac{e^{imk_0 z}}{m} J_0(k_0 r b) L_N\left(\frac{b^2}{\epsilon^2}\right) b\,\mathrm{d}b,$$

$$B_x^a = \sum \partial^2_{\bar{x}\bar{y}} \int_0^1 e^{-(b^2/\epsilon^2)} \frac{e^{imk_0 z}}{m} J_0(k_0 r b) L_N\left(\frac{b^2}{\epsilon^2}\right) b\,\mathrm{d}b,$$

$$B_y^a = \sum \left[\int_0^1 e^{-(b^2/\epsilon^2)} m e^{imk_0 z} J_0(k_0 r b) L_N\left(\frac{b^2}{\epsilon^2}\right) b\,\mathrm{d}b - \partial^2_{\bar{x}} \int_0^1 e^{-(b^2/\epsilon^2)} \frac{e^{imk_0 z}}{m} J_0(k_0 r b) L_N\left(\frac{b^2}{\epsilon^2}\right) b\,\mathrm{d}b \right],$$

$$B_z^a = i \sum \partial_{\bar{y}} \int_0^1 e^{-(b^2/\epsilon^2)} e^{imk_0 z} J_0(k_0 r b) L_N\left(\frac{b^2}{\epsilon^2}\right) b\,\mathrm{d}b.$$

This holds for arbitrary complex values of A_N, allowing for a large amount of flexibility in specifying the field profile. For any focal plane field distribution $f(\xi)\exp(-\xi)$, the constants A_N are simply the MacLaurin series coefficients, $A_N = [f^{(N)}(0)]/N!$, where $\xi = r^2/w_0^2$ and $f^{(N)}(\xi)$ is the Nth derivative of $f(\xi)$ with respect to ξ.

The fully symmetric flat-top fields can now be found by repeating the calculation with $B_y(z=0)$ having the form of Eq. (5) and averaging the two solutions. The real electric field components are then

$$E_x(x,y,z) = \frac{E_0}{\epsilon^2}\left(I_1 + \frac{x^2 - y^2}{k_0 r^3} I_2 + \frac{y^2}{r^2} I_3\right), \tag{6}$$

$$E_y(x,y,z) = \frac{E_0}{\epsilon^2} \frac{xy}{k_0 r^3}(2I_2 - k_0 r I_3), \tag{7}$$

$$E_z(x,y,z) = \frac{E_0}{\epsilon^2} \frac{x}{r} I_4. \tag{8}$$

The magnetic field is formally identical with the roles of x and y reversed, and the integrals I_n are defined as

$$I_1 = \sum_{N=0}^{\infty} \hat{A}_N \int_0^1 e^{-\zeta^2}(m + m^2)\sin(\phi_m) J_0(\Lambda) L_N(\zeta^2)\,\mathrm{d}m,$$

$$I_2 = \sum_{N=0}^{\infty} \hat{A}_N \int_0^1 e^{-\zeta^2} \sin(\phi_m) J_1(\Lambda) L_N(\zeta^2)\sqrt{1 - m^2}\,\mathrm{d}m,$$

$$I_3 = \sum_{N=0}^{\infty} \hat{A}_N \int_0^1 e^{-\zeta^2} \sin(\phi_m) J_0(\Lambda) L_N(\zeta^2)(1 - m^2)\,\mathrm{d}m,$$

$$I_4 = \sum_{N=0}^{\infty} \hat{A}_N \int_0^1 e^{-\zeta^2} \kappa(m)\cos(\phi_m) J_1(\Lambda) L_N(\zeta^2)\,\mathrm{d}m$$

for $\hat{A}_N = A_N N!$, $\Lambda = k_0 r\sqrt{1-m^2}$, $\zeta^2 = (1-m^2)/\epsilon^2$, $\phi_m = \omega_0 t - k_0 z m + \phi_0$, and $\kappa(m) = (1+m)\sqrt{1-m^2}$. This solution is formally identical to those derived previously as $N \to 0$, but now, however, the integration variable has been changed to $m = \sqrt{1-b^2}$ to eliminate the removable singularity present in Eqs. (1)–(3).[8,17]

Some ambiguity occurs when computing these fields as r approaches zero. In fact, this limit can be computed exactly for each of the field components. As one may expect by the symmetry of the system, the longitudinal (E_z, B_z) and secondary transverse (E_y, B_x) fields tend to zero while the primary transverse electric field component E_x obeys

$$\lim_{r \to 0} E_x = \frac{1}{4} \sum \int_0^1 e^{-\zeta^2} \sin\phi_m L_N(\zeta^2)(m + 1)^2\,\mathrm{d}m, \tag{9}$$

and B_y satisfies the same relation ensuring smooth, continuous fields. This on-axis integration for the asymmetric fields has been carried out in closed form, assuming a loose focus by Borghi *et al.*[22]

3. EXACT SERIES SOLUTION FOR A FLATTENED GAUSSIAN MODE LASER

As already noted, the integrals in Eqs. (6)–(8) have been derived previously for a purely Gaussian laser mode in this form by both Quesnel and Mora[8] and Varga and Török[17] and in asymmetric form by Cicchitelli *et al.*[1] In each case, the solution was presented only in integral form. The exact analytical solution of the related integrals from the asymmetric form has recently been derived by noting that they are in the form of Gegenbauer's finite integral.[43] This does, in fact, yield a field model identical to Eqs. (6)–(8) after symmetrization, including all flattened and annular Gaussian modes. The resulting field equations, however, are cumbersome. Here, an alternate solution following the same technique is presented now, evaluating the symmetric I_1–I_4 directly instead of the asymmetric integrals of Section 2. The simplicity of the resulting expressions for the electromagnetic field components, generated by only redefining the expansion coefficients thereby creating no additional runtime computational overhead, makes this an attractive alternative.

A. Fourier–Gegenbauer Formalism

Each of the integrals I_1–I_4 is of the general form,

$$\int_0^{\pi/2} f_n(\theta)\sin^{\mu+1/2}\theta J_{\mu-1/2}(k_0 r \sin\theta) e^{ik_0 z\cos\theta}\,\mathrm{d}\theta. \tag{10}$$

This possesses an exact analytical solution when the function $f_n(\theta)$ can be recast in a Fourier–Gegenbauer series, as described in Watson[47] or Kant.[48] To derive this solution, we first expand the function $f_n(\theta)$ using the orthogonal Gegenbauer polynomial basis

$$f_n(\theta) = \sum_{s=0}^{\infty} a_{s,0}^{\mu-1/2} C_s^{\mu}(\cos\theta), \tag{11}$$

where $C_s^{\mu}(t)$ are the Gegenbauer polynomials.[49] The expansion coefficients are defined as

$$a_{s,d}^{\mu-1/2} = N_s^{\mu-1/2} \int_0^{\pi/2} f_n(\theta)\cos^d\theta C_s^{\mu}(\cos\theta)\sin^{\mu+1/2}\theta \mathrm{d}\theta, \tag{12}$$

in which the proportionality constant $N_s^{\mu-1/2}$, derived from the orthogonality properties of the Gegenbauer polynomials, is

$$N_s^{\mu-1/2} = \left[\frac{2^{2\mu}(s+\mu)\Gamma^2(\mu)\Gamma(s+1)}{2\pi\Gamma(s+2\mu)}\right],$$

where $\Gamma(x)$ is the Γ-factorial function. Substituting the expansion of Eq. (11) into the general form of Eq. (10), the integration can be carried out directly, yielding

$$2\sum_{s=0}^{\infty} a_{s,0}^{\mu-1/2} i^s \left(\frac{r}{\rho}\right)^{\mu-1/2} C_s^{\mu}\left(\frac{z}{\rho}\right) j_{\mu-1/2+s}(k_0\rho), \tag{13}$$

where $\rho = \sqrt{r^2+z^2}$, $i=\sqrt{-1}$, and $j_n(x)$ is the nth-order spherical Bessel function of the first kind.[49] All that remains to complete the integration is to determine the values of the expansion coefficients. Thus, instead of evaluating Eq. (10), only Eq. (12) needs to be calculated.

The Gegenbauer polynomials arising in Eqs. (11) and (12) satisfy the recursion relation

$$sC_s^{\mu}(t) = 2(\mu+s-1)tC_{s-1}^{\mu}(t) - (2\mu+s-2)C_{s-2}^{\mu}(t)$$

for $s=2,3,4,\ldots$, where the first two polynomials are $C_0^{\mu}(t)=1$ and $C_1^{\mu}(t)=2\mu t$. Given this recursive definition, computing the coefficients in a simple closed form for all s is not trivial. Instead, consider $a_{0,d}^{\mu-1/2}$ for all $d=0,1,2,\ldots$. Following from the properties of the Gegenbauer polynomials, then,

$$a_{1,d}^{\mu-1/2} = 2\mu\left(\frac{N_1^{\mu-1/2}}{N_0^{\mu-1/2}}\right) a_{0,d+1}^{\mu-1/2}, \tag{14}$$

and the remaining coefficients are found from

$$a_{s,d}^{\mu-1/2} = \left[\frac{2(\mu+s-1)}{s}\right]\left(\frac{N_s^{\mu-1/2}}{N_{s-1}^{\mu-1/2}}\right) a_{s-1,d+1}^{\mu-1/2} - \left(\frac{2\mu+s-2}{s}\right) \times \left(\frac{N_s^{\mu-1/2}}{N_{s-2}^{\mu-1/2}}\right) a_{s-2,d}^{\mu-1/2} \tag{15}$$

for all $s=2,3,4,\ldots$, and $d=0,1,2,\ldots$. Thus computing the integrals having the form of Eq. (10) has finally been reduced to evaluating integrals of the form

$$a_{0,d}^{\mu-1/2} = N_0^{\mu-1/2} \int_0^{\pi/2} f_n(\theta)\cos^d\theta \sin^{\mu+1/2}\theta \mathrm{d}\theta \tag{16}$$

for $f_n(\theta)$, as defined by Eq. (10).

B. Gaussian Laser Fourier–Gegenbauer Solution

With the formalism of the solutions established, the details for each of the four integrals in Eqs. (6)–(8) can be worked out. First, the simpler pure Gaussian laser profile is worked out to illustrate the technique. Once this is complete, the result is extended to the general flattened Gaussian.

Each of the integrals I_1–I_4 are in the form of Eq. (10). Considering the order of the Bessel functions, the integrals I_1 and I_3 have $\mu=1/2$, and I_2 and I_4 imply $\mu=3/2$. To take full advantage of the similarities among these integrals, the integrals I_2 and I_4 are recast to a $\mu=1/2$ form such that

$$I_2 = -\frac{1}{k_0}\frac{\partial}{\partial r}\int_0^1 e^{-\zeta^2}\left(\frac{e^{i\phi_m}-e^{-i\phi_m}}{2i}\right) J_0(\Lambda)\mathrm{d}m,$$

$$I_4 = -\frac{1}{k_0}\frac{\partial}{\partial r}\int_0^1 e^{-\zeta^2}(m+1)\left(\frac{e^{i\phi_m}+e^{-i\phi_m}}{2}\right) J_0(\Lambda)\mathrm{d}m, \tag{17}$$

recalling that $\zeta^2=(1-m^2)/\epsilon^2$, $\Lambda=k_0 r\sqrt{1-m^2}$, and $\phi_m=\omega_0 t + \phi_0 - k_0 z m$. Now, as all of the integrals have been posed in a form such that $\mu=1/2$, all $\mu-1/2$ indices will henceforth be suppressed.

The simplest function is that of I_2, in which f_2 is given directly as

$$f_2(\cos\theta) = e^{-\zeta^2} = e^{(\cos^2\theta-1)/\epsilon^2},$$

where the variable has been changed according to $m=\cos\theta$ to match the formalism of the Subsection 3.A. Following the model outlined above, this function is expanded in a Fourier–Gegenbauer series with $\mu=1/2$, and the $s=0$ and $d=0,1,2,\ldots$, expansion coefficients are from Eq. (16),

$$\hat{b}_{0,d} = \frac{1}{d}(-i\epsilon)^{d+1}\gamma\left(\frac{d+1}{2},-\frac{1}{\epsilon^2}\right)e^{-1/\epsilon^2}, \tag{18}$$

where $\gamma(a,x)$ is the lower incomplete Γ function defined by[49]

$$\gamma(a,x) = \int_0^x t^{a-1}e^{-t}\mathrm{d}t \xrightarrow{x\to\infty} \Gamma(a),$$

where $\Gamma(a)$ is again the Γ-factorial function: $\Gamma(n+1)=n!$ for integer n. The $s>0$ terms then follow from Eqs. (14) and (15) as

$$\hat{b}_{1,d} = 3\hat{b}_{0,d+1},$$

$$\hat{b}_{s,d} = \left(\frac{2s-1}{s}\right)\left[\hat{b}_{s-1,d+1} - \left(\frac{s-1}{2s-3}\right)\hat{b}_{s-2,d}\right]. \tag{19}$$

Thus, to determine the first S expansion coefficients in the Fourier–Gegenbauer series, each of the constants $\hat{b}_{0,d}$ must be computed for $d=0,1,2,\ldots,S-1$.

The other integrals I_1, I_3, and I_4 simply multiply the driver function $f_2(\theta)$ by powers of $m=\cos\theta$. For example, $f_1(\theta)=\exp(-\zeta^2)(m+m^2)=(\cos\theta+\cos^2\theta)f_2(\theta)$. From the definition of the coefficients [cf. Eq. (12)] then, multiplying by the kth power of $m = \cos\theta$ is equivalent to incrementing d by k. Thus, the expansion coefficients arising from $f_1(\theta)$, $\hat{a}_{s,d}$, can be simply related to those of $f_2(\theta)$ by employing Eq. (12):

$$N_s \int_0^1 f_2(\theta)(\cos^{d+1}\theta + \cos^{d+2}\theta) C_s^{1/2}(\cos\theta) \mathrm{d}(\cos\theta)$$

$$= N_s \int_0^1 f_1(\theta)\cos^d \theta C_s^{1/2}(\cos\theta)\mathrm{d}(\cos\theta),$$

yielding the relation,

$$\hat{a}_{s,d} = \hat{b}_{s,d+1} + \hat{b}_{s,d+2}. \tag{20}$$

Carrying on this process for the remaining integrals, the expansion coefficients for each integral can be easily related to those from $f_2(\theta)$, yielding

$$\hat{c}_{s,d} = \hat{b}_{s,d} - \hat{b}_{s,d+2},$$

$$\hat{d}_{s,d} = \hat{b}_{s,d} + \hat{b}_{s,d+1}, \tag{21}$$

for f_3 and f_4, respectively. Therefore, to carry S terms in each of the four series, only $S+2$ constants need to be known: namely, $\hat{b}_{0,0}, \hat{b}_{0,1}, \ldots, \hat{b}_{0,S+1}$. The rest follow from the known recursions of Eqs. (19). In fact, this is the same number required in the asymmetric solution referenced above.[43] As an example, Fig. 1 shows the four coefficients for $w_0 = \lambda_0$. In this case, only 20 terms are necessary to evaluate each integral. In fact, as the focusing tightens, these series converge more quickly, as described in Subsection 3.C.

Finally, the exact symmetric Maxwell wave-equation solution for a Gaussian focused beam, given in Eqs. (6)–(8), can be stated in terms of the Fourier–Gegenbauer expansion and the associated coefficients:

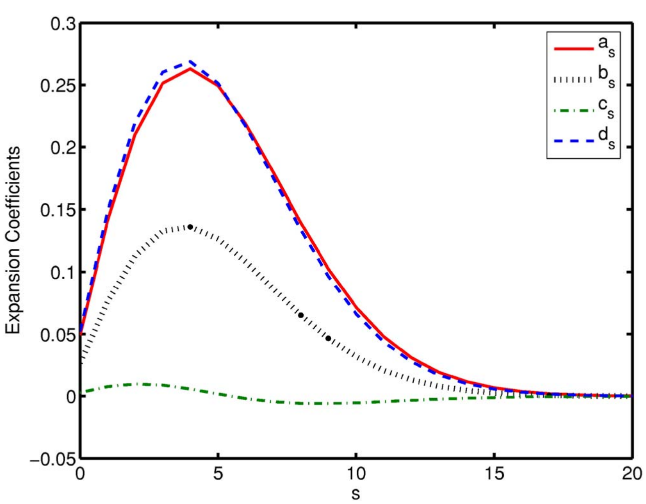

Fig. 1. (Color online) Four sets of expansion coefficients, $\hat{a}_{s,0}$, $\hat{b}_{s,0}$, $\hat{c}_{s,0}$, and $\hat{d}_{s,0}$, for the case of $w_0 = \lambda_0$ ($\epsilon = 1/\pi \approx 0.3183$).

$$E_x(\mathbf{x},t) = E_0\left(\frac{2}{\epsilon^2}\right)\sum_{s=0}^{\infty} \sin\varphi_s \left\{ \left(\hat{a}_{s,0} + \frac{y^2}{r^2}\hat{c}_{s,0}\right) C_s^{1/2}\left(\frac{z}{\rho}\right) j_s(k_0\rho) - \left(\frac{x^2-y^2}{k_0 r^3}\right)\hat{b}_{s,0}\partial_{\bar{r}}\left[C_s^{1/2}\left(\frac{z}{\rho}\right) j_s(k_0\rho)\right]\right\},$$

$$E_y(\mathbf{x},t) = -E_0\left(\frac{2}{\epsilon^2}\right)\left(\frac{xy}{k_0 r^3}\right) \times \sum_{s=0}^{\infty} \sin\varphi_s \left\{ 2\hat{b}_{s,0}\partial_{\bar{r}}\left[C_s^{1/2}\left(\frac{z}{\rho}\right) j_s(k_0\rho)\right] + (k_0 r)\hat{c}_{s,0} C_s^{1/2}\left(\frac{z}{\rho}\right) j_s(k_0\rho)\right\},$$

$$E_z(\mathbf{x},t) = -E_0\left(\frac{2}{\epsilon^2}\right)\left(\frac{x}{r}\right) \times \sum_{s=0}^{\infty} \cos\varphi_s \left\{ \hat{d}_{s,0}\partial_{\bar{r}}\left[C_s^{1/2}\left(\frac{z}{\rho}\right) j_s(k_0\rho)\right]\right\},$$

where $\varphi_s = \omega_0 t + \phi_0 - s\pi/2$. The magnetic field is identical following the transformation $(x,y) \to (y,x)$, and the derivative terms can be simply evaluated, giving

$$\partial_{\bar{r}}\left[C_s^{1/2}\left(\frac{z}{\rho}\right) j_s(k_0\rho)\right] = \left(\frac{sz}{k_0 r\rho}\right)\left[\left(\frac{z}{\rho}\right) C_s^{1/2}\left(\frac{z}{\rho}\right) - C_{s-1}^{1/2}\left(\frac{z}{\rho}\right)\right] j_s(k_0\rho) + \left(\frac{r}{\rho}\right) C_s^{1/2}\left(\frac{z}{\rho}\right) \times \left[\frac{s j_{s-1}(k_0\rho) - (s+1) j_{s+1}(k_0\rho)}{2s+1}\right],$$

adopting the convention that $C_{-1}^{1/2}(x) \equiv 0$.

C. Limits, Comments, and Discussion

As this solution is derived from an orthogonal polynomial representation instead of through perturbative corrections to the paraxial wave equation, no requirements are made explicitly on the magnitude of the diffraction angle, ϵ. In fact, in direct contrast to these perturbative solutions, the series expression derived here converges more quickly for tighter focusing rather than looser focusing. The number of terms required for the Fourier–Gegenbauer series to converge is found to be $S \sim 20(w_0/\lambda_0)$. For example, when $w_0 = \lambda_0$, only 20 terms are required in each series, but when $w_0 = 10\lambda_0$, 200 terms are required. This follows from the form of the functions, $f_n(\theta)$ modeled by the Fourier–Gegenbauer expansion in the integrals I_1–I_4. Figure 2 shows the case of $f_2(\theta)$ for several values of ϵ. When $w_0 \gtrsim 10\lambda_0$, the functions $f_n(\theta)$ become sharply peaked at $\theta = 0$, making them difficult to express using this technique. As the waist w_0 approaches the laser wavelength λ_0, however, the function spreads out in θ and becomes increasingly easy to capture through such a Fourier–Gegenbauer model. This creates an ideal situation. The perturbative nonparaxial series solutions derived previously[13–16] have been used with great success for waists of the order of several wavelengths, but as w_0

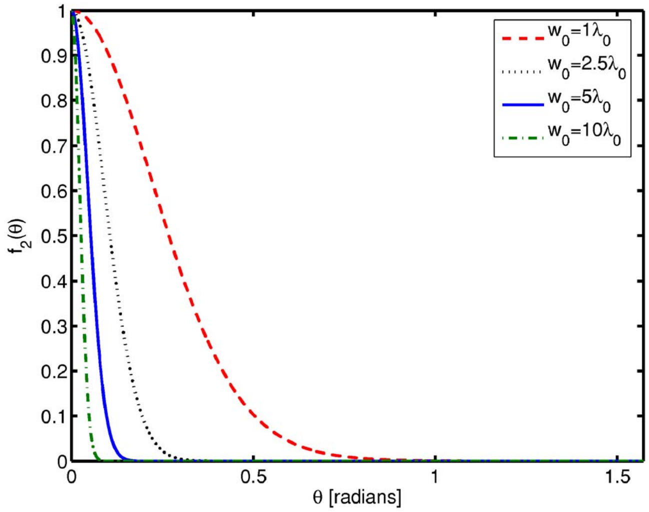

Fig. 2. (Color online) Transform function $f_2(\theta)=\exp[(\cos^2\theta-1)/\epsilon^2]$ from I_2 for several values of $\epsilon=\lambda_0/\pi w_0$. Note that as the focusing loosens, the laser beam becomes directed only along $\hat{\mathbf{z}}$, corresponding here to $\theta=0$. That is, the diffraction lessens as expected.

$\rightarrow\lambda_0$, the expansion parameter ϵ is no longer small. In that case, this Fourier–Gegenbauer solution now becomes the solution of choice, converging quickly while satisfying the Maxwell wave equation exactly.

A common application of such a vector electromagnetic field model arises in solving the equation of motion $\mathbf{F}=q(\mathbf{E}+\boldsymbol{\beta}\times\mathbf{B})$ either for a single particle interacting with the fields or in conjunction with a Maxwell solver in a plasma fluid or particle-in-cell code, in which the fields are imposed as boundary conditions. Numerically evaluating the integrals in Eqs. (6)–(8) for each time step of a simulation is often computationally prohibitive. This series solution takes full advantage of the formal similarities of these integrals to simplify the calculation of the field components and lower the computation time by introducing redundancy of form. All four series contain the spherical Bessel functions of the first kind, $j_s(x)$, ranging from the order of $s=0$ to $s=S$ when S terms are retained in each series. Thus, only $S+1$ Bessel functions need be computed for each interation, a computationally inexpensive process as they are related by a simple arithmetic recursion. Similarly, only S Gegenbauer polynomials are required, and they are also related by a simple recursion. This solution also contains $3S$ expansion coefficients. Thus, the computational load in terms of spherical Bessel function, Gegenbauer polynomials, and expansion coefficients required is identical to the model introduced previously,[43] but the final field expressions are much simpler.

The limit of this solution as $r\rightarrow 0$ is stated in integral form in Eq. (9). In terms of this analytical solution, the integral becomes

$$\lim_{r\rightarrow 0} E_x=\epsilon^{-2}E_0\sum_{s=0}^{\infty}(2\hat{a}_{s,0}+\hat{c}_{s,0})j_s(k_0z)\sin\varphi_s.$$

This leads to the interesting result that due to the symmetrization of the solution, the amplitude of the wave at the focus—i.e., $(x,y,z)=(0,0,0)$—is not, in general, equal to E_0 but is given by

$$\lim_{\rho\rightarrow 0} E_x=\left(\frac{2\hat{a}_{0,0}+\hat{c}_{0,0}}{\epsilon^2}\right)E_0$$
$$=\left[\frac{1}{4}(3-2e^{-(1/\epsilon^2)})-i\left(\frac{2-\epsilon^2}{8\epsilon}\right)\right.$$
$$\left.\times e^{-(1/\epsilon^2)}\gamma\left(\frac{1}{2},-\frac{1}{\epsilon^2}\right)\right]E_0. \tag{22}$$

The magnitude of the field at the focus differs as much as 3.4% from E_0 as the spot size $2w_0\rightarrow\lambda_0$. This is shown explicitly in Fig. 3. For large spot sizes, this effect is negligible, and $\lim_{\rho\rightarrow 0}E_x=E_0$. Borghi *et al.* have also calculated the Gaussian field distribution on the laser axis analytically,[22] but that solution failed to capture this effect as their boundary condition only specified a transverse Gaussian electric field, and no corresponding Gaussian magnetic field condition was imposed. This solution was, in fact, the asymmetric form.

D. Flattened Gaussian Solution

With the purely Gaussian case worked out, the general flattened Gaussian fields follow naturally and, in fact, can be defined in terms of the simpler Gaussian case. Higher-order non-Gaussian terms added to the angular spectrum integrals and, hence, the functions $f_n(m)$, take the form of Laguerre polynomials in $\zeta^2=(1-m^2)/\epsilon^2$. Recalling the series definition of the unassociated Laguerre polynomials and employing the binomial theorem, the flattened Gaussian driver functions $f_n^{\mathrm{N}}(m)$ generated by the Nth-order Laguerre polynomial are easily related to the Gaussian drivers $f_n(\theta)$ by

$$f_n^{\mathrm{N}}(m)=f_n(m)L_N(\zeta^2)$$
$$=\sum_{l=0}^{N}\sum_{k=0}^{l}\frac{(-1)^{l+N-k}N!\,\epsilon^{-2l}}{(N-l)!(l-k)!k!}[f_n(m)m^{2N-2k}].$$

The only difference introduced by the Laguerre polynomials is to multiply each term by $m^{2N-2k}=\cos^{2N-2k}\theta$. As the

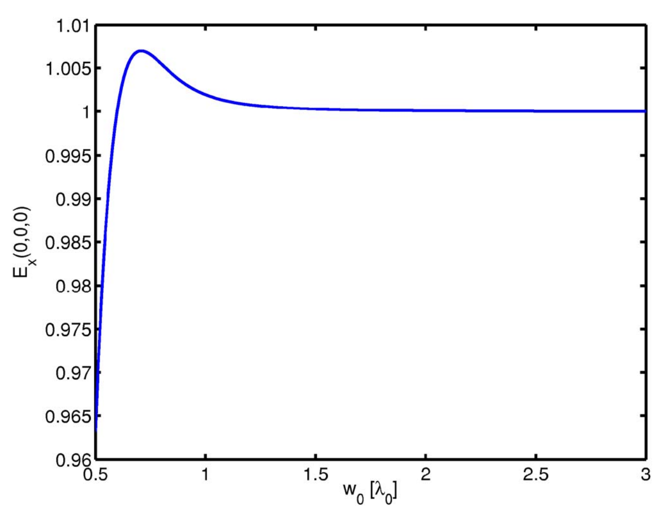

Fig. 3. (Color online) Value of E_x/E_0 at the focus as a function of the spot size, w_0. This follows as $(2a_{0,0}^0+b_{0,0}^0)\epsilon^{-2}$ from Eq. (22).

expansion coefficients are again defined by Eq. (12) this is formally equivalent to simply incrementing d by $2N-2k$. Thus, the expansion coefficients for $f_2^N(\theta)$, $\hat{b}_{s,d}^N$ can be related to the Gaussian terms $\hat{b}_{s,d}$ by

$$\hat{b}_{s,d}^N = \sum_{l=0}^{N} \sum_{k=0}^{l} (-1)^{l+N-k} \frac{N! \epsilon^{-2l} \hat{b}_{s,d+2N-2k}}{(N-l)!(l-k)!k!}, \tag{23}$$

and the corresponding coefficients for I_1, I_3, and I_4 again obey the relationships given in Eqs. (20) and (21) for each N.

Thus, including up to the Nth order of the flattened Gaussian only necessitates the calculation of $2N$ additional terms of $\hat{b}_{0,d}^0$, meaning that, if S terms are to be retained in each series, and N flattened Gaussian terms will be included, only the coefficients $\hat{b}_{0,0}^0$, $\hat{b}_{0,1}^0, \ldots, \hat{b}_{0,S+2N+1}^0$ need to be computed. The remaining terms are computed using the recursions of Eqs. (14), (15), and (23).

This formal symmetry extends to the full field expressions for the exact flattened Gaussian electric field

$$E_x(\mathbf{x},t) = E_0\left(\frac{2}{\epsilon^2}\right)\sum_{N=0}^{\infty}\hat{A}_N\sum_{s=0}^{\infty} \sin\varphi_s\left\{\left(\hat{a}_{s,0}^N + \frac{y^2}{r^2}\hat{c}_{s,0}^N\right)\right.$$
$$\times C_s^{1/2}\left(\frac{z}{\rho}\right)j_s(k_0\rho) - \left(\frac{x^2-y^2}{k_0 r^3}\right)$$
$$\left.\times \hat{b}_{s,0}^N \partial_{\bar{r}}\left[C_s^{1/2}\left(\frac{z}{\rho}\right)j_s(k_0\rho)\right]\right\},$$

$$E_y(\mathbf{x},y) = -E_0\left(\frac{2}{\epsilon^2}\right)\left(\frac{xy}{k_0 r^3}\right)$$
$$\times \sum_{N=0}^{\infty}\hat{A}_N\sum_{s=0}^{\infty} \sin\varphi_s\left\{2\hat{b}_{s,0}^N\partial_{\bar{r}}\left[C_s^{1/2}\left(\frac{z}{\rho}\right)j_s(k_0\rho)\right]\right.$$
$$\left.+ (k_0 r)\hat{c}_{s,0}^N C_s^{1/2}\left(\frac{z}{\rho}\right)j_s(k_0\rho)\right\},$$

$$E_z(\mathbf{x},t) = -E_0\left(\frac{2}{\epsilon^2}\right)\left(\frac{x}{r}\right)$$
$$\times \sum_{N=0}^{\infty}\hat{A}_N\sum_{s=0}^{\infty} \cos\varphi_s\left\{\hat{d}_{s,0}^N\partial_{\bar{r}}\left[C_s^{1/2}\left(\frac{z}{\rho}\right)j_s(k_0\rho)\right]\right\}.$$

and again, the magnetic field components are identical save for the rotation $(x,y)\rightarrow(y,x)$.

4. CONCLUSION

The six symmetric electromagnetic field components of a focused laser with a general, flattened Gaussian transverse profile have been derived *exactly* in integral form by the use of Fourier transforms. Such a derivation has, in fact, been performed previously for a purely Gaussian profile[1,8,17] and for a flattened Gaussian.[43] Under tight focusing conditions—i.e., $w_0 \lesssim 10\lambda_0$—the integrals are difficult and computationally expensive to evaluate, and for larger spot sizes become nearly impossible because of the sharply peaked integrand. A cumbersome series solution valid for small spot sizes has also recently been developed by making use of a Fourier–Gegenbauer expansion. In this paper, a similar approach has been taken, but by making a better choice in defining the expansion coefficients, the complexity of the resulting field expressions for both a Gaussian focal plane profile and the more general flattened Gaussian has been greatly reduced, without the addition of *any* computational overhead. That is, the same number of Gegenbauer polynomials, spherical Bessel functions, and expansion coefficients must be computed to retain equal numbers of terms in the expansion.

Interestingly, when the limiting value of the fields is computed at the focus—that is, at $(x,y,z)=(0,0,0)$—the laser amplitude is found to deviate from the nominal E_0 by as much as $\sim 3.4\%$. This is a result of the symmetrization of the solution; that is, the averaging of the separate E_x and B_y flattened Gaussian boundary condition fields.

The analytical focused field model derived in this paper allows for direct and accurate modeling of laser interactions as the spot size approaches the laser wavelength for a host of beam profiles. In the standard Hermite–Gaussian solutions, the wave equation is solved through a perturbative series expansion that requires more terms to converge as the spot size decreases. The series solution presented here, in fact, provides a full vector field model with the flexibility to model a wide array of beam profiles while requiring fewer and fewer terms as the spot size approaches a single wavelength, thereby making it attractive for many problems of current interest, including electron acceleration,[50–52] monochromatization of polychromatic electron beams,[7] laser micromachining,[34] and direct acceleration of electrons in vacuum.[1,4,9–11,53,54]

For some time, paraxial and series representations have sufficed, but as laser focusing and intensities reach ever-higher levels, an accurate and robust field model is essential. The exact solution derived here satisfies that requirement and represents a true technological convergence as computing power has also risen in coincidence with laser and optical limits, now allowing such exact solutions to be evaluated and applied to practical laser problems.

ACKNOWLEDGMENTS

The authors gratefully acknowledge support for this work from the National Science Foundation and from the Chemical Sciences, Geosciences, and Biosciences Division of the Office of Basic Energy Sciences, U.S. Department of Energy. S. M. Sepke also thanks Matthew Rever for many helpful and insightful discussions. S. M. Sepke was also supported in part by Sandia National Laboratories, Department of Defense-Subcontracts, award 26588.

S. M. Sepke's e-mail address is ssepke@unlserve.unl.edu.

REFERENCES

1. L. Cicchitelli, H. Hora, and R. Postle, "Longitudinal field components for laser beams in vacuum," Phys. Rev. A **41**, 3727–3732 (1990).
2. H. Hora, *Physics of Laser Driven Plasmas* (Wiley, 1981).
3. H. Hora, *Laser Plasma Physics* (SPIE, 2000).

4. H. Hora, M. Hoelss, W. Scheid, J. W. Wang, Y. K. Ho, F. Osman, and R. Castillo, "Acceleration of electrons in vacuum by lasers and the accuracy principle of nonlinearity," in *High-Power Lasers in Energy Engineering*, K. Mima, G. L. Kulcinski, and W. Hogan, eds., Proc. SPIE **3886**, 145–156 (2000).
5. B. W. Boreham and B. Luther-Davies, "High-energy electron acceleration by ponderomotive forces in tenuous plasmas," J. Appl. Phys. **50**, 2533–2538 (1979).
6. B. W. Boreham and H. Hora, "Debye length discrimination of nonlinear laser forces acting on electrons in tenuous plasmas," Phys. Rev. Lett. **42**, 776–779 (1979).
7. S. Banerjee, S. Sepke, R. Shah, A. Valenzuela, A. Maksimchuk, and D. Umstadter, "Optical deflection and temporal characterization of ultrafast laser-produced electron beams," Phys. Rev. Lett. **95**, 035004 (2005).
8. B. Quesnel and P. Mora, "Theory and simulation of the interaction of ultraintense laser pulses with electrons in vacuum," Phys. Rev. E **58**, 3719–3732 (1998).
9. A. Maltsev and T. Ditmire, "Above threshold ionization and in tightly focused, strongly relativistic laser fields," Phys. Rev. Lett. **90**, 053002 (2003).
10. H. Hora, W. Scheid, T. Hauser, Y. Kato, Y. Kitagawa, K. Mima, and T. Yamanaka, "Free wave laser acceleration of electrons and consequences for the Umstadter experiment," in *Proceedings of the 13th International Conference on Laser Interaction and Related Plasma Phenomena*, Aip Conf. Proc. No. 406, G. Miley and E. M. Campbell, eds. (AIP, 1997), p. 495.
11. S. Masuda, M. Kando, H. Kotaki, and K. Nakajima, "Suppression of electron scattering by the longitudinal components of tightly focused laser fields," Phys. Plasmas **12**, 013102 (2005).
12. A. E. Siegman, *Lasers* (University Science Books, 1986).
13. M. Lax, W. H. Louisell, and W. B. McKnight, "From Maxwell to paraxial wave optics," Phys. Rev. A **11**, 1365–1370 (1975).
14. L. W. Davis, "Theory of electromagnetic beams," Phys. Rev. A **19**, 1177–1179 (1979).
15. J. P. Barton and D. R. Alexander, "Fifth-order corrected electromagnetic field components for a fundamental Gaussian beam," J. Appl. Phys. **66**, 2800–2802 (1989).
16. J. X. Wang, W. Sheid, M. Hoelss, and Y. K. Ho, "Fifth-order corrected field descriptions of the Hermite–Gaussian (0,0) and (0,1) mode laser beam," Phys. Rev. E **64**, 066612 (2001).
17. P. Varga and P. Török, "The Gaussian wave solution of Maxwell's equations and the validity of scalar wave approximation," Opt. Commun. **152**, 108–118 (1998).
18. M. Koenig, B. Faral, J. M. Boudenne, D. Batani, A. Benuzzi, and S. Bossi, "Optical smoothing techniques for shock wave generation in laser-produced plasmas," Phys. Rev. E **50**, R3314–R3317 (1994).
19. V. V. Goloviznin, P. W. van Amersfoort, N. E. Andreev, and V. I. Kirsanov, "Self-resonant plasma wake-field excitation by a laser pulse with a steep leading edge for particle acceleration," Phys. Rev. E **52**, 5327–5332 (1995).
20. Y. Kawamura, Y. Itagaki, K. Toyoda, and S. Namba, "A simple optical device for generating square flat-top intensity irradiation from a Gaussian laser beam," Opt. Commun. **48**, 44–46 (1983).
21. D. Shafer, "Gaussian to flat-top intensity distributing lens," Opt. Laser Technol. **14**, 159–160 (1982).
22. R. Borghi, A. Ciattoni, and M. Santarisiero, "Exact axial electromagnetic field for vectorial Gaussian and flattened Gaussian boundary distributions," J. Opt. Soc. Am. A **19**, 1207–1211 (2002).
23. C. J. R. Sheppard and S. Saghafi, "Flattened light beams," Opt. Commun. **132**, 144–152 (1996).
24. Y. Li, "Light beams with flat-topped profiles," Opt. Lett. **27**, 1007–1009 (2002).
25. R. Borghi, "Elegant Laguerre–Gaussian beams as a new tool for describing axisymmetric flattened Gaussian beams," J. Opt. Soc. Am. A **18**, 1627–1633 (2001).
26. A. Fulop, G. Bourdet, J. C. Chanteloup, C. Dambrine, S. Ferre, S. L. Moal, A. Pichot, G. L. Touze, H. Yu, and Z. Zhao, "Diode pumped Yb:YAG V-shape unstable super-Gaussian laser resonators for 10 Hz to 100 Joule clase laser," Proc. SPIE **5708**, 20–31 (2005).
27. T. Lehecka, R. H. Lehmberg, A. V. Deniz, K. A. Gerber, S. P. Obenschain, C. J. Pawley, M. S. Pronko, and C. A. Sullivan, "Production of high energy, uniform focal profiles with the Nike laser," Opt. Commun. **117**, 485–491 (1995).
28. T. Y. Cherezova, S. S. Chesnokov, L. N. Kaptsov, and A. V. Kudryashov, "Super-Gaussian laser intensity output formation by means of adaptive optics," Opt. Commun. **155**, 99–106 (1998).
29. W. C. Yen, C. T. Huang, H. P. Liu, and L. P. Lee, "A Nd:YAG laser with a flat-top beam profile and constant divergence," Opt. Laser Technol. **29**, 57–61 (1997).
30. X. H. Lu, X. M. Chen, L. Zhang, and D. J. Xue, "High-order Bessel–Gaussian beam and its propagation properties," Chin. Phys. Lett. **20**, 2155–2157 (2003).
31. K. Zhu, H. Tang, X. Sun, X. Wang, and T. Liu, "Flattened multi-Gaussian light beams with an axial shadow generated through superposing Gaussian beams," Opt. Commun. **207**, 29–34 (2002).
32. Y. Cai and Q. Lin, "The elliptical Hermite–Gaussian beam and its propagation through paraxial systems," Opt. Commun. **207**, 139–147 (2002).
33. A. Shevchenko, S. C. Buchter, N. V. Tabiryan, and M. Kaivola, "Creation of a hollow laser beam using self-phase modulation in a nematic liquid crystal," Opt. Commun. **232**, 77–82 (2004).
34. I. Manek, Y. B. Ovchinnikov, and R. Grimm, "Generation of a hollow laser beam for atom trapping using an axicon," Opt. Commun. **147**, 67–70 (1998).
35. A. Pertovaara, T. J. Morrow, and K. L. Casey, "Cutaneous pain and detection thresholds to short CO_2 laser pulses in humans: evidence on afferent mechanisms and the influence of varying stimulus conditions," Pain **34**, 261–269 (1988).
36. S. DeSilvestri, P. Laporta, V. Magni, and O. Svelto, "Solid-state laser unstable resonators with tapered reflectivity mirrors: the super-Gaussian approach," IEEE J. Quantum Electron. **QE-24**, 1172–1177 (1988).
37. H. Mao and D. Zhao, "Different models for a hard-aperture function and corresponding approximate analytical propagation equations of a Gaussian beam through an apertured optical system," J. Opt. Soc. Am. A **22**, 647–653 (2005).
38. Y. Li, "New expressions for flat-topped light beams," Opt. Commun. **206**, 225–234 (2002).
39. F. Gori, "Flattened Gaussian beams," Opt. Commun. **107**, 335–341 (1994).
40. R. Potvliege, "Waveletlike basis function approach to the propagation of paraxial beams," J. Opt. Soc. Am. A **17**, 1043–1047 (2000).
41. M. Santarsiero and R. Borghi, "Correspondence between super-Gaussian and flattened Gaussian beams," J. Opt. Soc. Am. A **16**, 188–190 (1999).
42. V. Bagini, R. Borghi, F. Gori, A. M. Pacileo, M. Santarsiero, D. Ambrosini, and G. S. Spagnolo, "Propagation of axially symmetric flattened Gaussian beams," J. Opt. Soc. Am. A **13**, 1385–1385 (1996).
43. S. Sepke and D. Umstadter, "Exact analytical solution for the vector electromagnetic field of Gaussian, flattened Gaussian, and annular Gaussian laser modes," Opt. Lett. **31**, 1447–1449 (2006).
44. R. Haberman, *Elementary Applied Partial Differential Equations With Fourier Series and Boundary Value Problems*, 3rd ed. (Prentice Hall, 1997).
45. J. W. Goodman, *Introduction to Fourier Optics* (McGraw-Hill, 1968).
46. G. P. Agrawal and D. N. Pattanayak, "Gaussian beam propagation beyond the paraxial approximation," J. Opt. Soc. Am. **69**, 575–578 (1979).
47. G. N. Watson, *A Treatise on the Theory of Bessel Functions* (Cambridge U. Press, 1980).
48. R. Kant, "An analytical solution of vector diffraction for

focusing optical systems," J. Mod. Opt. **40**, 337–347 (1993).

49. M. Abramowitz and I. A. Stegun, eds., *Handbook of Mathematical Functions*, 12th ed. (Dover, 1972).
50. S. P. D. Mangles, C. D. Murphy, Z. Najmudin, A. G. R. Thomas, J. L. Collier, A. E. Dangor, E. J. Divall, P. S. Foster, J. G. Gallacher, C. J. Hooker, D. A. Jaroszynski, A. J. Langley, W. B. Mori, P. A. Norreys, F. S. Tsung, R. Viskup, B. R. Walton, and K. Krushelnick, "Monoenergetic beams of relativistic electrons from intense laser-plasma interactions," Nature **431**, 535–538 (2004).
51. C. G. R. Geddes, C. Toth, J. van Tilborg, E. Esarey, C. B. Schroeder, D. Bruhwiler, C. Nieter, J. Cary, and W. P. Leemans, "High-quality electron beams from a laser wakefield accelerator using plasma channel guiding," Nature **431**, 538–541 (2004).
52. J. Faure, Y. Glinec, A. Pukhov, S. Kiselev, S. Gordienko, E. Lefebvre, J.-P. Rousseau, F. Burgy, and V. Malka, "A laser-plasma accelerator producing monoenergetic electron beams," Nature **431**, 541–544 (2004).
53. U. Mohideen, M. H. Sher, H. W. K. Tom, G. D. Aumiller, O. R. Wood, R. R. Freeman, J. Boker, and P. H. Bucksbaum, "High intensity above-threshold ionization of He," Phys. Rev. Lett. **71**, 509–512 (1993).
54. G. Malka, E. Lefebvre, and J. L. Miquel, "Experimental observation of electrons accelerated in vacuum to relativistic energies by a high-intensity laser," Phys. Rev. Lett. **78**, 3314–3317 (1997).